SENSOR ORIENTATION FOR HIGH-RESOLUTION SATELLITE IMAGERY

H.B. Hanley, T. Yamakawa, C.S. Fraser

Department of Geomatics, University of Melbourne, Victoria 3010 Australia
hanley@sunrise.sli.unimelb.edu.au, yamakawa@sunrise.sli.unimelb.edu.au, c.fraser@unimelb.edu.au

Commission I, WG I/5

KEY WORDS: high-resolution satellite imagery, Ikonos *Geo* imagery, sensor orientation, high-accuracy geopositioning

ABSTRACT:

An investigation into the use of alternative sensor orientation models and their applicability for block adjustment of high-resolution satellite imagery is reported. Ikonos *Geo* imagery has been employed in the investigation, and since the explicit camera model and precise exterior orientation information required to apply conventional collinearity-based models is not provided with Ikonos data, alternative sensor orientation models are needed. The orientation models considered here are bias-corrected rational functions (with vendor-supplied rational polynomial coefficients) and the affine projection model. Test results arising from the application of the alternative image orientation/triangulation models within two multi-strip, stereo blocks of *Geo* imagery are reported. These results confirm that *Geo* imagery can yield three-dimensional geopositioning to pixel and even sub-pixel accuracy over areas of coverage extending well beyond the nominal single scene area for Ikonos. The accuracy achieved is not only consistent with expectations for rigorous sensor orientation models, but is also readily attainable in practice with only a small number of high-quality ground control points.

1. INTRODUCTION

Over the past two years the photogrammetry research team at the Department of Geomatics, University of Melbourne has been investigating sensor orientation/triangulation models for high-resolution satellite imagery. In this work, the focus has been fundamentally on two modelling approaches that require very modest ground control, but do not require explicit access to the 'camera model'. The first of these is the Rational Function Model (RFM[*]) with additional parameters for bias correction, and the second is the affine projection model. Work to date with Ikonos *Geo* imagery has produced sub-metre three-dimensional accuracy from stereo- and three-image coverage (eg Fraser et al., 2001; 2002a,b; Fraser & Hanley, 2002).

The area used in the initial evaluation of these two models was the Melbourne Ikonos test field (Hanley & Fraser, 2001), which had the advantage of containing 50 highly accurate ground control points (GCPs), but the disadvantage of being only about 7 x 7 km in area. Given that one of the features of alternative sensor orientation models is perceived to be that they display more significant accuracy shortcomings as the area of coverage increases, it was deemed desirable to test the proposed models over areas comprising multiple, overlapping scenes. The authors were fortunate in gaining access to two comprehensive Ikonos *Geo* data sets, one covering San Diego and the other of an area in Mississippi. For convenience, these data sets will be simply referred to as the San Diego and Mississippi blocks. Both blocks of imagery provided an excellent opportunity to test alternative sensor orientation models over a much larger area than was imaged within the Melbourne Test Field.

---

[*] We will refer to the rational function coefficients that are supplied with the Ikonos imagery by the familiar term of RPCs, whereas we use the abbreviation RFM for the rational function model itself. The use of RPCs implies that the coefficients represent a sensor orientation that is essentially an accurate reparameterisation of the rigorous sensor model.

2. TEST DATA

2.1 The San Diego Block

This block, shown in Fig. 1, comprised three overlapping strips of stereo *Geo* imagery and covered an area of 50x50 km, although the ground control array of 62 GCPs was confined to a 24 x 24km area of central San Diego (the data originally supplied by Space Imaging included 147 GCPs, however not all of these were suitable for precise image measurement). The present investigation is thus restricted to the 580km^2 area containing the GCPs, which displayed an elevation range of 220m. The left most image strip had three-fold coverage consisting of a forward/nadir/reverse triplet recorded in a single orbit, whereas the middle and right strips each comprised a forward/reverse stereo pair. The left and middle strips overlapped by about 2.5 km and shared eight common GCPs, while the middle and right strips overlapped by only 400m and had no common GCPs. The accuracy of the GCPs is nominally sub-metre.

2.2 The Mississippi Block

Shown in Fig. 2 is the 6-strip configuration of the approximately 50 x 60km Mississippi block (see also Dial & Grodecki, 2002), which comprised 36 GCPs and 16 measured tie points. As distinct from the San Diego block, the authors had access to the measured image and GCP coordinates, and to the RPCs for the 12 images, but not to the imagery. The analysis was therefore confined to this measurement data set alone. An advantage of the Mississippi block was that is allowed an investigation of the merits and shortcomings of alternative orientation models over such a large area, namely 2800 km^2. A disadvantage was that there was no quantitative estimate of accuracy for either the GCPs or the supplied image coordinate observations.

3. RATIONAL FUNCTIONS

Due to its focus on Ikonos imagery, the following discussion of rational functions is confined to the so-called terrain-independent, forward RFM that describes the object-to-image

space transformation. The 80 RPCs supplied with the imagery (now via the *Geo*-Ortho Kit or Ikonos stereo products), along with 10 scale and offset terms, serve to accurately reparameterise the rigorous sensor orientation (Grodecki, 2001). The RFM is given as:

$$F_1 = l_n = \frac{Num_L(U,V,W)}{Den_L(U,V,W)}$$
$$F_2 = s_n = \frac{Num_S(U,V,W)}{Den_S(U,V,W)} \tag{1}$$

where

$$Num_L(U,V,W)_j = a_1 + a_2V + a_3U + a_4W + a_5VU$$
$$+ a_6UW + a_7UW + a_8V^2 + a_9U^2$$
$$+ a_{10}W^2 + a_{11}UVW + a_{12}V^3$$
$$+ a_{13}VU^2 + a_{14}VW^2 + a_{15}V^2U$$
$$+ a_{16}U^3 + a_{17}UW^2 + a_{18}V^2W$$
$$+ a_{19}U^2W + a_{20}W^3 \tag{2}$$

$$Den_L(U,V,W)_j = b_1 + b_2V + \ldots + b_{19}U^2W + b_{20}W^3$$
$$Num_S(U,V,W)_j = c_1 + c_2V + \ldots + c_{19}U^2W + c_{20}W^3$$
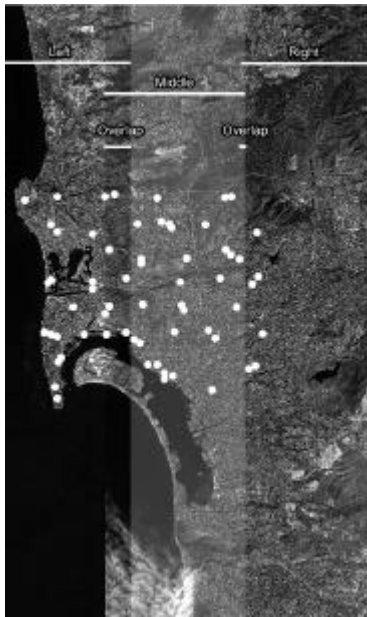$$Den_S(U,V,W)_j = d_1 + d_2V + \ldots + d_{19}U^2W + d_{20}W^3$$

Figure 1: San Diego block showing GCP locations.

Here, l_n, s_n are the normalised (offset and scaled) line, sample image coordinates and U, V, W are the corresponding object point coordinates, which refer to normalised latitude, longitude and height. That is,

$$l_n = \frac{l - LineOffset}{LineScale} \qquad U = \frac{f - LatitudeOffset}{LatitudeScale}$$
$$s_n = \frac{s - SampleOffset}{SampleScale} \qquad V = \frac{l - LongitudeOffset}{LongitudeScale} \tag{3}$$
$$W = \frac{h - HeightOffset}{HeightScale}$$

where (l, s) are measured line, sample coordinates and (f, l, h) are the geographical coordinates of the ground point.
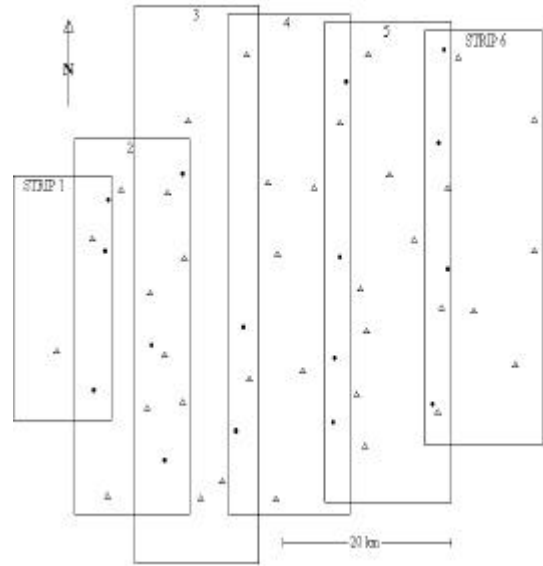

Figure 2. Configuration of Mississippi block showing stereo strips, GCPs (▣) and tie points (●).

In order to perform an image-to-object point transformation, either stereo image coverage or known height in the case of a single image is required. In stereo and multi-image networks (>2 images), ground coordinates can be obtained from the RFM via an indirect least-squares model of the form

$$\begin{pmatrix} v_l \\ v_s \end{pmatrix}_{ij} = A_{ij} \begin{pmatrix} df \\ dl \\ dh \end{pmatrix}_j + \begin{pmatrix} l^o - l \\ s^o - s \end{pmatrix}_{ij} \tag{4}$$

where v_l and v_s are observational residuals in pixels; df, dl, dh are corrections to approximate values for the object point coordinates in latitude, longitude and ellipsoidal height; l^o, s^o are the image coordinates corresponding to the approximate object coordinates (obtained via Eq. 1); and A_{ij} is the matrix of partial derivatives of the functions in Eq. 1 with respect to f, l, h. Within the least squares solution it is necessary to use l, s, f, l and h instead of their normalized counterparts to account for different scales and offsets between images.

Eq. 4 offers a practical method for 3D geopositioning from RPCs, however it does not incorporate the means to accommodate exterior orientation biases which are inherent in satellite image products derived without the aid of ground control. Tests have shown that biases of as much as 70m are possible. Biases in image space coordinates for a given image can be computed through a direct comparison of measured image coordinates with those determined from measured GCPs through application of Eq. 1 (eg Fraser et al, 2002a,b; Fraser & Hanley, 2002).

4. RPC BIAS COMPENSATION

4.1 Modelling Biases in Image Space

Plotted in Fig. 3 are the RPC bias values for selected points in the nadir image of the left strip of the San Diego block. The vectors show the near-constant difference between measured image points and the corresponding positions obtained by projecting the GCP position into the image via Eq. 1. The

plots of image space biases for the remaining strips show a similar pattern, though the magnitude and direction of the bias vectors in each image can be expected to vary. Figure 4 shows the biases obtained for all GCPs within the Mississippi block for the left-hand images of each stereo pair. The strip-invariant nature of the biases is noteworthy in the figure.

Tables 1 and 2 list the corresponding mean values and standard errors for all image biases, for all strips in both blocks. The image-coordinate discrepancies, Dl and Ds, for the San Diego and Mississippi blocks reach 4 and 16 pixels, respectively. Nevertheless, the standard errors for all images are well under one pixel, suggesting a high degree of invariance of image point biases within an image. The standard errors are generally higher in the Mississippi block, for which there was unfortunately no quantitative information available to the authors regarding the accuracy of either the image measurements or the GCP coordinates.
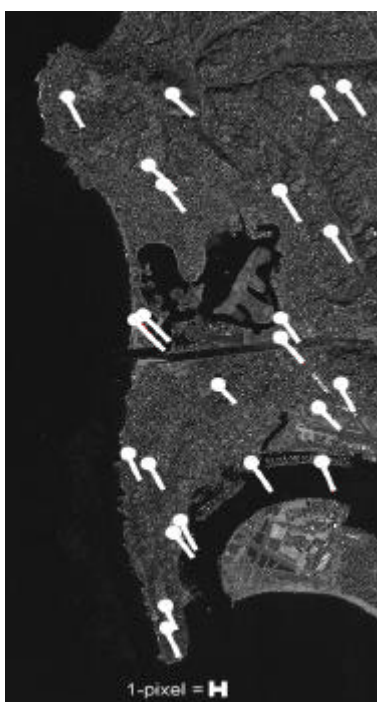

Figure 3. Plot of RPC biases for an image of the San Diego block.
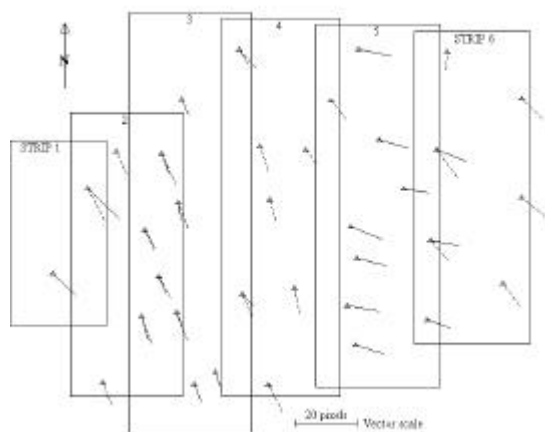

Figure 4. Plots of RPC image point biases for the Mississippi block; left-hand stereo images only.

From the plots of Figs. 3 and 4, and the results listed in Tables 1 and 2, it is apparent that a good starting point in any attempt to compensate for RPC biases would be through application of a translation of image point coordinates, an approach that has previously been investigated by Fraser & Hanley (2002), Fraser et al. (2002a,b) and Dial & Grodecki (2002). We now consider this approach.

Table 1. Mean and standard error values for the RPC bias-induced image point shifts Dl and Ds obtained for 63 GCPs in the San Diego block.

Image	Mean Δl	Mean Δs	σ_l	σ_s
Left 1	3.69	2.58	0.19	0.19
Left 2	3.76	2.01	0.20	0.19
Left 3	4.07	1.81	0.17	0.19
Middle 1	3.30	2.50	0.20	0.17
Middle 2	3.89	2.59	0.21	0.21
Right 1	3.35	4.01	0.32	0.29
Right 2	3.54	3.06	0.35	0.25

Table 2. Mean and standard error values for the RPC bias-induced image point shifts Dl and Ds obtained for the 36 GCPs in the Mississippi block.

Image	Mean Δl	Mean Δs	σ_l	σ_s
Strip 1L	7.98	1.76	0.33	0.30
Strip 1R	3.67	2.71	0.32	0.27
Strip 2L	6.55	5.20	0.43	0.43
Strip 2R	7.91	7.79	0.46	0.43
Strip 3L	2.21	8.15	0.32	0.31
Strip 3R	3.69	8.91	0.28	0.30
Strip 4L	12.15	9.03	0.35	0.35
Strip 4R	2.21	2.30	0.37	0.34
Strip 5L	7.11	3.58	0.29	0.31
Strip 5R	7.96	4.24	0.35	0.32
Strip 6L	-0.64	-2.83	0.34	0.32
Strip 6R	15.82	9.01	0.32	0.30

Under the assumption that RPC biases manifest themselves for all practical purposes as image coordinate shifts, a model for bias compensation that comprises one offset parameter per image coordinate can be derived through an extension of Eq. 2, as shown in Fraser et al. (2002a):

$$\begin{pmatrix} v_l \\ v_s \end{pmatrix}_{ij} = \begin{pmatrix} \dfrac{\partial F_1}{\partial f} & \dfrac{\partial F_1}{\partial l} & \dfrac{\partial F_1}{\partial h} & 1 & 0 \\ \dfrac{\partial F_2}{\partial f} & \dfrac{\partial F_2}{\partial l} & \dfrac{\partial F_2}{\partial h} & 0 & 1 \end{pmatrix}_{ij} \begin{pmatrix} df_j \\ dl_j \\ dh_j \\ A_{0i} \\ B_{0i} \end{pmatrix} + \begin{pmatrix} l^o - l \\ s^o - s \end{pmatrix}_{ij} \quad (5)$$

Here, A_{0i} and B_{0i} are image coordinate perturbations that are common to image i. In a 'bundle adjustment' of a stereo strip or block via Eq. 4, only one GCP is necessary for absolute geopositioning. The merit of Eq. 4 lies in both its simplicity and in its applicability to multi-image triangulation using the Ikonos RPCs for images that exhibit very different bias characteristics.

If the possibility of drift effects in the along- and cross-track directions are also taken into account (Dial & Grodecki, 2002), Eq. 4 is expanded to the form:

$$\begin{pmatrix} v_l \\ v_s \end{pmatrix}_{ij} = \begin{pmatrix} \dfrac{\partial F_1}{\partial f} & \dfrac{\partial F_1}{\partial l} & \dfrac{\partial F_1}{\partial h} & 1 & 0 & l & 0 \\[2ex] \dfrac{\partial F_2}{\partial f} & \dfrac{\partial F_2}{\partial l} & \dfrac{\partial F_2}{\partial h} & 0 & 1 & 0 & s \end{pmatrix}_{ij} \begin{pmatrix} df_j \\ dl_j \\ dh_j \\ A_{0i} \\ B_{0i} \\ A_{1i} \\ B_{1i} \end{pmatrix} + \begin{pmatrix} l^o - l \\ s^o - s \end{pmatrix}_{ij} \quad (6)$$

where, in addition to the bias parameters A_{0i} and B_{0i}, parameters A_{1i} and B_{1i} representing drift are introduced. In a block adjustment via Eq. 5, at least two GCPs are necessary and depending on the degree of strip overlap and tie point distribution in a block, two GCPs per strip would be a recommended minimum. Although the two bias parameters A_0 and B_0 and drift terms A_1 and B_1 are modelled as image space perturbations, the very long focal length (10m) and narrow view angle (0.93^o) of the Ikonos sensor means that what is taking place is a lateral shift and drift of the sensor platform in two orthogonal directions, i.e. a correction to exterior orientation which, although positional, is more likely in reality to be compensating for sensor attitude errors. This is explained in more detail in Dial & Grodecki (2002).

The results of simulation studies conducted by Dial & Grodecki (2002) suggest that the drift terms will not assume significance until the *Geo* strip is at least 50km long, and even over this length the magnitude of the drift effect reaches a maximum of about 0.3 pixel. Thus, it would be expected that drift terms might have an impact on the achievable RPC-block adjustment accuracy in the Mississippi block, whereas their effect in the San Diego block could be expected to be negligible.

4.2 Application of RPC Bias Compensation

Tables 3 and 4 provide summaries of results obtained in the application of the RPC bias compensation in 'bundle adjustments' of the San Diego and Mississippi blocks, using the models of both Eqs. 5 and 6, for a number of different GCP configurations. The listed RMS values of image space residuals suggest an overall image measurement precision of about $1/3^{rd}$ of a pixel, which is consistent with expectations. It is noteworthy in the San Diego block that the drift terms have virtually no impact on the image space residuals, suggesting – as anticipated – that any drift that is present in the 24km strip sections is 'within the noise'. This is also largely the case in the Mississippi block, though here there is an improvement in image space residuals resulting from application of Eq. 6.

In terms of object point positioning accuracy it is noteworthy that Eq. 5, with image offset terms only, generally produces the better results. Accuracies (RMS 1-sigma) in planimetry of better than 1 pixel are obtained in both cases, with height accuracies being around 1.2-1.5 pixels. Application of Eq. 6 leads to an accuracy degradation, especially in height in the San Diego block and in planimetry in the Mississippi block, suggesting a degree of overparameterisation.

Given that the authors do not have an estimate of the precision of the measured GCPs in either block, or the accuracy of image coordinate observations in the Mississippi block, results at the 1-metre accuracy level are seen as quite

satisfactory, and certainly good enough to demonstrate the effectiveness of the RPC bias compensation approach in block sizes exceeding 1000km^2.

Table 3. Results of Bias-Compensated Bundle Adjustment of the San Diego Block.

Model (GCP config.)	Image Residual RMS (pixels)	RMS of chkpt residuals	
		S_{XY}	S_Z (m)
Eq. 4 – shift terms only			
1 (lower left)	0.30	0.72	1.29
1 (upper right)	0.30	1.02	1.26
4 (corners)	0.31	0.70	1.46
6 (corners + 2 middle)	0.33	0.63	1.23
Eq. 5 – shift and drift			
2 (lower left upper right)	0.29	0.91	1.38
2 (upper left lower right)	0.29	1.29	1.86
4 (corners)	0.29	1.25	1.57
6 (corners + 2 middle)	0.31	0.83	1.35

Table 4. Results of Bias-Compensated Bundle Adjustment of the Mississippi Block.

Model (GCP config.)	Image Residual RMS(pixels)	RMS of chkpt residuals	
		S_{XY}	S_Z (m)
Eq. 4 – shift terms only			
1 (lower left)	0.40	0.90	1.57
1 (upper right)	0.41	0.89	1.26
4 (corners)	0.41	0.94	1.26
6 (corners + 2 middle)	0.42	0.95	1.17
Eq. 5 – shift and drift			
2 (lower left upper right)	0.31	2.33	1.21
2 (upper left lower right)	0.31	2.43	1.90
4 (corners)	0.31	2.19	0.98
6 (corners + 2 middle)	0.32	1.00	0.95

In the case of the bias-only runs (Eq. 5), the role of the GCPs is to effect an image coordinate translation and thus their location within the scene is of no real consequence. The addition of further GCPs makes no contribution to the geometric strength of the triangulation process per se. Instead the extra control points simply provide more information from which to evaluate an appropriate 'average' image coordinate correction. From the RMS values of ground checkpoint discrepancies listed in Tables 3 and 4, it can be seen that there is no clear link between the accuracy attained and the location or number of GCPs. Nevertheless, with the use of redundant control points one can be more confident about the reliability of the geopositioning process.

5. GENERATION OF BIAS-CORRECTED RPCS

The ability to determine the bias parameters A_0 and B_0 is very useful, but of more utility is the incorporation of the bias compensation into the originally supplied RPCs. This would then allow bias-free application of RPC-positioning without any reference to additional correction terms. Fortunately, it turns out that this bias compensation is a straightforward matter, the bias-corrected RPCs for any image being developed via the following process.

Extending Eq. 1 with the bias parameters leads to

$$l_n + A_{0n} = \frac{Num_L(U,V,W)}{Den_L(U,V,W)}$$
$$s_n + B_{0n} = \frac{Num_S(U,V,W)}{Den_S(U,V,W)}$$

(7)

where A_{0n} and B_{0n} are related to A_0 and B_0 by the following expressions:

$$A_{0n} = \frac{A_0}{LineScale} \quad \text{and} \quad B_{0n} = \frac{B_0}{SampleScale}$$

Eq. 7 can then be written as

$$l_n = \frac{Num_L^C(U,V,W)}{Den_L(U,V,W)}$$
$$s_n = \frac{Num_S^C(U,V,W)}{Den_S(U,V,W)}$$

(8)

where

$$Num_L^C(U,V,W) = (a_1 - b_1 A_{0n}) + (a_2 - b_2 A_{0n}) \cdot V +$$
$$(a_3 - b_3 A_{0n}) \cdot U + ... +$$
$$(a_{20} - b_{20} A_{0n}) \cdot W^3$$

(9)

$$Num_S^C(U,V,W) = (c_1 - d_1 B_{0n}) + (c_2 - d_2 B_{0n}) \cdot V +$$
$$(c_3 - d_3 B_{0n}) \cdot U + ... +$$
$$(c_{20} - d_{20} B_{0n}) \cdot W^3$$

Corrected RPCs that take into account bias and drift (A_1 and B_1) can be developed in a similar manner. It is anticipated, however, that there would be few users who would need to apply the drift terms, given that they do not assume any practical significance until the image strip length is well over 50km in length.

A software system, *Barista*, has been developed to perform the necessary generation of bias-corrected RPCs. This system allows interactive measurement of selected image points and the necessary GCP(s). It also includes computation of the bias parameters for any number of images, from any number of object points, and it carries out the generation of corrected RPCs in a file format identical to that originally supplied with the Ikonos imagery. This file is thus suited to utilisation with standard photogrammetric workstations that support stereo restitution via Ikonos RPCs, and it will facilitate bias-free 3D ground point determination.

6. THE AFFINE MODEL

The RFM with vendor-supplied RPCs is an effective alternative to collinearity-based sensor orientation models. For Ikonos *Geo* imagery, however, there is an extra cost associated with the provision of RPCs, which can reach $US30/km² for international users (Space Imaging, 2002). Indeed, in some markets, for example Japan, RPCs are not available at all with Ikonos imagery. There is therefore a considerable incentive to develop a practical sensor orientation model that has no requirement whatsoever for camera or exterior orientation parameters, but does need

some ground control. The authors have investigated a number of such models, notably the well-known DLT, an affine projection model and an affine-perspective model (affine in line direction and perspective in sample direction). Studies with *Geo* imagery of the smaller Melbourne testfield (eg Fraser et al., 2001, 2002a; Yamakawa et al., 2002) suggest that of these alternative orientation models, the affine model shows the most promise. In the following section we report on the application of the affine model to the much larger San Diego and Mississippi blocks.

Although the affine model can be justified in terms of the narrow view angle of the Ikonos sensor, the model is nevertheless a special case of the RFM. Thus, the following equations for the affine model are given in RPC terms as follows:

$$l_n = \frac{Num_L(U,V,W)}{Den_L(U,V,W)}$$
$$s_n = \frac{Num_S(U,V,W)}{Den_S(U,V,W)}$$

(10)

where

$$Num_L(U,V,W)_j = a_1 + a_2 V + a_3 U + a_4 W$$
$$Den_L(U,V,W)_j = 1$$
$$Num_S(U,V,W)_j = c_1 + c_2 V + c_3 U + c_4 W$$
$$Den_S(U,V,W)_j = 1$$

(11)

Once again, the image line and sample coordinates are offset-normalised, as are the object space coordinates. Although the offsetting and normalisation is not required, we have chosen to be consistent with RPC terminology because there is then the potential that the affine coefficients can be provided in a format the same as 'standard RPCs' and so can be directly employed with a photogrammetric workstation. There is one difficulty associated with this idea, however, especially in the case of long image strips, where it is generally not advisable to have the (U,V,W) coordinates representing normalised (f, l, h). Even with two additional parameters comprising quadratic correction terms, the affine model cannot effectively account for the non-linear nature of the geographical coordinates, especially longitude, which closely corresponds to the across-track direction.

To a much lesser extent the same is true for Cartesian coordinates in the case of strips of around 50km in length and the authors experience is that a standard 8-parameter affine model yields the best results when the chosen object space coordinate system is UTM. If a local Cartesian system is adopted, the affine model benefits from the inclusion of two additional parameters, namely a V^2 term in both the line and sample expressions. In the following discussion, we report only the results achieved with a model of eight parameters per strip and normalised UTM ground coordinates with ellipsoidal heights. Also, there is no initial perspective-to-affine image transformation (see Fraser et al, 2001).

In the implementation of the affine projection model for Ikonos orientation/triangulation, all affine parameters are recovered simultaneously along with (U,V,W) ground point coordinates in a process analogous to photogrammetric bundle adjustment. By taking advantage of prior knowledge of the satellite's position in orbit (from the azimuth and elevation angles provided in the metadata file), and

transforming all GCP positions to a common height plane, the 8-term model can be effectively reduced to six parameters, as has been described by Baltsavias et al. (2001).

The normal scenario for block formation with Ikonos imagery is to have a small overlap between strips, for example 10%. This geometric configuration unfortunately offers the prospect of adding via tie points additional signal to model affine distortion only in the along-track direction. Thus, it is generally warranted to provide the necessary minimum of 4 GCPs for each strip in the affine block adjustment computation. The GCP configurations selected for the testing within the San Diego and Mississippi blocks reflected this requirement, and strips contained from four to six GCPs.

In the case of San Diego, the GCPs were real GPS-surveyed ground points and thus the affine triangulation allowed an assessment of absolute accuracy. In the Mississippi block, however, some of the selected GCPs were actually points that were measured only in the imagery, their ground coordinates having been determined through the RPC bias-compensated block adjustment procedure previously outlined. This was unavoidable given the number of ground points available (recall that the imagery was not provided) and it meant that the results in the Mississippi block indicated accuracy with respect to the RPC triangulation, which effectively corresponded to the optimal possible solution.

Table 5 summarises the results obtained in the affine model approach for both blocks. Because of the relatively few control/checkpoints in the right-hand strip of the San Diego imagery, the affine model was applied only to the block comprising the left-hand and central strips. Similarly, in the case of Mississippi only four strips were included because of a shortage of checkpoints in the outer two strips. The results in the table show that the affine model applied to the multi-strip block configurations can produce object point positioning accuracy to the same level as achieved with bias-corrected RPCs, namely sub-pixel accuracy in planimetry and close to 1-pixel accuracy in height.

Table 5. Results of Block Adjustment via the Affine Model, with ground coordinates in UTM.

Block, GCP configuration	Image Residual RMS (pixels)	RMS of checkpoints S_{XY}	S_Z (m)
San Diego (9 GCPs, 47 Chk pts.)	0.39	0.76	1.03
Mississippi (15 GCPs, 25 Chk pts.)	0.26	0.79	1.13

The attainment of accuracy equivalent to the bias-corrected RPC model is the single most significant outcome of the investigation into the affine approach, because it demonstrates that long strips (greater than the nominal 22km scene length) can be accommodated without loss of model fidelity. Image coordinate residuals remain at the 0.3 pixel level and the object space accuracy is reasonably homogeneous across the entire area of the block. As has been stated on the occasion of the success of the affine model

within the 7 x 7km Melbourne testfield (Fraser et al., 2002a): The finding that such a straightforward 8-parameter linear model can produce geopositioning accuracy on a par with that from the 80-parameter RPC model (after bias removal) is very encouraging for the practitioner. Use of local Cartesian (X,Y,Z) instead of UTM GCP coordinates degraded the results to $S_{XY} = 1.0$m and $S_Z = 1.9$m in the Mississippi block. The corresponding values in the San Diego block were $S_{XY} = 0.7$m and $S_Z = 1.3$m, which demonstrates the adverse influence of longer strip length when Cartesian coordinates are employed.

7. CONCLUSIONS

Given the equivalence of the results obtained by the RPC and Affine models in the San Diego and Mississippi blocks, the question as to whether one should employ the empirical affine sensor orientation model or RPCs might well reduce to a matter of economics. The affine model requires more ground control (let's say 6-8 points per strip would be advisable), but *Geo* RPCs come at a price premium that could well exceed the cost of establishing and measuring the GCPs and carrying out the affine model computation. The answer to the question is left to the user, who of course would need the facilities to handle both approaches, for example via a software system such as the mentioned *Barista* system. One issue is clear, both approaches yield accuracy results equivalent to the much more expensive *Pro* and *Precision* range of Ikonos products.

As has been mentioned, one apparent shortcoming with the affine model applied to longer *Geo* image strips is that there is a fall-off in accuracy if the chosen (U,V,W) coordinate system relates to normalised latitude, longitude and height. Thus, although the affine coefficients can be formatted such that any digital photogrammetric work station would accept them as Ikonos RPCs (of the 80 coefficients, all but 10 would be zero) the accuracy obtained in stereo restitution might fall short of expectations. In this situation, a case could be made for generating a new set of 80 RPCs using the affine model as the 'rigorous model'. This 'black-box' operation could be made invisible to the Ikonos *Geo* image user.

8. ACKNOWLEDGEMENTS

9. REFERENCES

Baltsavias, E., Pateraki, M. and L. Zhang, 2001. Radiometric and geometric evaluation of Ikonos *GEO* images and their use for 3D building modelling. *Proc. Joint ISPRS Workshop "High Resolution Mapping from Space 2001"*, Hanover, 19-21 September, 21p. (on CDROM).

Dial, G. and J. Grodecki, 2002. Block adjustment with rational polynomial camera models. *Proceedings ASPRS Annual Meeting*, Washington, DC, 22-26 May, 9 pages (on CD-ROM).

Fraser, C.S., Hanley, H.B. and T. Yamakawa, 2001. Sub-metre geopositioning with Ikonos *Geo* imagery. *Proc. Joint ISPRS Workshop "High Resolution Mapping from Space 2001"*, Hanover, 19-21 Sept., 8p. (on CDROM).

Fraser, C.S., Hanley, H.B. and T. Yamakawa, 2002a. 3D positioning accuracy of Ikonos imagery. *Photogramm. Record,* 17(99): 465-479.

Fraser, C.S., Hanley, H.B. and T. Yamakawa, 2002b. High-precision geopositioning from Ikonos satellite imagery. *Proceedings ASPRS Annual Meeting, Washington*, DC, 22-26 May, 9 pages (on CDROM).

Fraser, C.S. and H.B. Hanley, 2002. Bias compensation in rational functions for Ikonos satellite imagery. *Photogrammetric Engineering & Remote Sensing,* 11 pages (in press).

Grodecki, J., 2001. Ikonos stereo feature extraction - RPC approach. *Proc. ASPRS Annual Conference*, St. Louis, 23-27 April, 7 p. (on CDROM).

Hanley, H.B. and C.S. Fraser, 2001. Geopositioning accuracy of Ikonos imagery: indications from 2D transformations. *Photogrammetric Record*, 17(98): 317-329.

Space Imaging (2002) Company web site, accessed 5 August 2002: http://www.spaceimaging.com.

Yamakawa, T., Fraser, C.S. and H.B. Hanley, 2002. Orientation of IKONOS satellite imagery via alternative orientation models. *Proc. of JSPRS Conference*, Tokyo, 3-5 July, 201-204 (in Japanese).